NACA

# RESEARCH MEMORANDUM

## PRESSURE DISTRIBUTIONS ON THIN CONICAL BODY OF ELLIPTIC CROSS SECTION AT MACH NUMBER 1.89

By Stephen H. Maslen

Lewis Flight Propulsion Laboratory
Cleveland, Ohio



NATIONAL ADVISORY COMMITTEE
FOR AERONAUTICS

WASHINGTON
January 20, 1949

NACA RM No. E8K05

NATIONAL ADVISORY COMMITTEE FOR AERONAUTICS

RESEARCH MEMORANDUM

# PRESSURE DISTRIBUTIONS ON THIN CONICAL BODY OF ELLIPTIC CROSS SECTION AT MACH NUMBER 1.89

By Stephen H. Maslen

## SUMMARY

An investigation was conducted to determine the pressure distribution on a conical body of elliptic cross section at a Mach number of 1.89. Experimental data are presented for a range of angles of yaw from -16° to 16° and angles of attack from -10° to 10°.

As the angle of flow deflection was increased, the deviation from experiment of the theoretical pressure distribution slightly increased, although agreement was satisfactory over the entire range of calculations. Comparison of the complete equation for pressure coefficient (that is, the equation including all the perturbation velocity components) with the equation usually used in connection with the linearized theory indicated that the terms usually neglected appreciably alter the predicted values of the pressure coefficient. Although the complete equation gave better agreement with experiment for the elliptic cone investigated than did the linearized equation, the opposite result was found when a similar comparison with the exact results of Taylor and Maccoll was made. The excellent agreement between experiment and linearized theory may therefore be fortuitous.

## INTRODUCTION

Aircraft designers are currently in need of a reliable means of estimating loads on body contours that might be used as fuselages of supersonic airplanes. Several methods have been available for the theoretical calculation of force distribution over bodies of revolution, as well as considerable experimental data for checking such calculations (for example, references 1 to 5). Recently, a theoretical method for calculating the pressure distribution over conical bodies of noncircular cross section has also become available (reference 6).

An experimental investigation was undertaken at the NACA Lewis laboratory to check theoretical calculations for a conical body of elliptic cross section. The results are compared with calculations based on the linearized theory given in reference 6.

## SYMBOLS

The following symbols are used in this report:

| | |
|---|---|
| $C_p$ | pressure coefficient |
| K | constant proportional to source strength |
| M | Mach number |
| m | slope of line source with respect to x-axis |
| U | free-stream velocity |
| $U_r$ | radial perturbation-velocity component (cylindrical coordinate) |
| $U_x$ | axial perturbation-velocity component |
| $U_x'$ | perturbation-velocity component parallel to free-stream direction |
| $U_\theta$ | tangential perturbation-velocity component (cylindrical coordinate) |
| $x,r,\theta$ | cylindrical coordinates |
| $\alpha$ | angle of attack, degrees |
| $\beta$ | cotagent of Mach angle, $\sqrt{M^2-1}$ |
| $\gamma$ | ratio of specific heats |
| $\delta$ | angular position of line source measured from $\theta = \pi/2$ plane |
| $\Psi$ | angle of yaw, degrees |

## APPARATUS AND PROCEDURE

The cone was mounted on a support body in the Lewis 18-by-18-inch supersonic tunnel, as shown in figure 1. The support body was a sweptback strut fastened to the tunnel wall by means of a lock nut. From a previous calibration, the Mach number in the vicinity of the model was 1.89 with a maximum deviation of ±0.5 percent.

A sketch of the model showing the dimensions and the location of the pressure orifices is presented in figure 2. The body was machined of brass and the nose was finished to a sharp point. Orifices of 0.010-inch diameter were drilled normal to the body surface. Pressures were photographically recorded on a multiple-tube manometer board using tetrabromoethane as a fluid.

The model, mounted as shown in figure 1, and the strut were turned together to obtain data for the body in yaw. In order to obtain the desired angle of attack, the model was rotated 90° relative to the strut and the angle was varied by turning the strut. By use of a vernier, the angle could be read to within 2.5 minutes. Pressures were recorded every 0.5° up to ±16° angle of yaw at an angle of attack of 0° and ±10° angle of attack at an angle of yaw of 0°.

## THEORY

A method of calculating the pressure distribution about a cone of arbitrary cross section by means of a series of line sources is presented in reference 6. The following perturbation velocities result from such sources:

$$U_x = -K\left(\frac{1}{1-(m\beta)^2}\cos^{-1}\left\{\frac{1-m\frac{r}{x}\beta^2\sin(\theta-\delta)}{\sqrt{\left[1-m\frac{r}{x}\beta^2\sin(\theta-\delta)\right]^2-\left[1-\left(\frac{r\beta}{x}\right)^2\right]\left[1-(m\beta)^2\right]}}\right\}\right.$$

$$\left.-\frac{(m\beta)^2-m\frac{r}{x}\beta^2\sin(\theta-\delta)}{\left[1-m\frac{r}{x}\beta^2\sin(\theta-\delta)\right]^2-\left[1-\left(\frac{r\beta}{x}\right)^2\right]\left[1-(m\beta)^2\right]}\sqrt{\frac{1-\left(\frac{r\beta}{x}\right)^2}{1-(m\beta)^2}}\right) \qquad (1)$$

$$U_r = K\beta\left(\frac{m\beta\sin(\theta-\delta)}{1-(m\beta)^2}\cosh^{-1}\left\{\frac{1-m\frac{r}{x}\beta^2\sin(\theta-\delta)}{\sqrt{\left[1-m\frac{r}{x}\beta^2\sin(\theta-\delta)\right]^2-\left[1-\left(\frac{r\beta}{x}\right)^2\right]\left[1-(m\beta)^2\right]}}\right\}\right.$$

$$\left.+\frac{\frac{r\beta}{x}\left[1-(m\beta)^2\right]-\left[1-m\frac{r}{x}\beta^2\sin(\theta-\delta)\right]m\beta\sin(\theta-\delta)}{\left[1-m\frac{r}{x}\beta^2\sin(\theta-\delta)\right]^2-\left[1-\left(\frac{r\beta}{x}\right)^2\right]\left[1-(m\beta)^2\right]}\sqrt{\frac{1-\left(\frac{r\beta}{x}\right)^2}{1-(m\beta)^2}}\right) \qquad (2)$$

$$U_\theta = Km\beta^2 \cos(\theta-\delta)\left(\frac{1}{1-(m\beta)^2}\cosh^{-1}\left\{\frac{1 - m\frac{r}{x}\beta^2 \sin(\theta-\delta)}{\sqrt{\left[1 - m\frac{r}{x}\beta^2 \sin(\theta-\delta)\right]^2 - \left[1 - \left(\frac{r\beta}{x}\right)^2\right]\left[1 - (m\beta)^2\right]}}\right\}\right.$$

$$\left. - \frac{1 - m\frac{r}{x}\beta^2 \sin(\theta-\delta)}{\left[1 - m\frac{r}{x}\beta^2 \sin(\theta-\delta)\right]^2 - \left[1 - \left(\frac{r\beta}{x}\right)^2\right]\left[1 - (m\beta)^2\right]}\sqrt{\frac{1 - \left(\frac{r\beta}{x}\right)^2}{1 - (m\beta)^2}}\right) \tag{3}$$

The boundary condition of the flow is

$$\frac{U_r}{U} - \left(\frac{1}{r}\frac{\partial r}{\partial \theta}\right)\frac{U_\theta}{U} - \frac{r}{x}\frac{U_x}{U} = \frac{r}{x} \tag{4}$$

From integration of the Bernoulli equation for isentropic flow, the pressure coefficient becomes

$$C_p = \frac{2}{\gamma M^2}\left(\left\{1 - \frac{\gamma-1}{\gamma}M^2\left[\frac{2U_x}{U} + \left(\frac{U_x}{U}\right)^2 + \left(\frac{U_r}{U}\right)^2 + \left(\frac{U_\theta}{U}\right)^2\right]\right\}^{\frac{\gamma}{\gamma-1}} - 1\right) \tag{5}$$

In connection with the linearized theory, this relation is usually approximated as

$$C_p = -2\frac{U_x}{U} \tag{6}$$

Theoretical calculations for several bodies showed that the pressure distributions predicted by the two relations were enough different that the approximate equation omits more terms from the exact relation than is justified. Therefore, although the use of the exact relation for the pressure coefficient may be mathematically inconsistent with the approximations of the linearized theory, it has been used in the theoretical calculations presented herein, except where otherwise noted.

For systematic calculations of flows at angles of attack or yaw, the procedure outlined in reference 6 is too tedious. A simpler means is to consider the flow slightly inclined with respect to the x-axis rather than to move the body relative to this axis. This procedure of turning the flow rather than the body in obtaining the angle-of-attack solution means that the Mach cones are assumed to follow the body rather than the flow. Although in the actual case the Mach cones would follow the flow more closely than the body, this assumption was made to facilitate numerical calculations. If the angle of attack or yaw is kept small, such an assumption should introduce little error. The boundary condition was obtained in the same manner as in reference 6.

$$U_r - \left(\frac{1}{r}\frac{\partial r}{\partial \theta}\right)U_\theta - \frac{r}{x}U_x = U\left[\frac{\frac{r}{x}}{\sqrt{\tan^2\alpha + \tan^2\Psi + 1}}\right.$$

$$-\frac{1}{\sqrt{1+\cot^2\Psi\sec^2\alpha}}\left(\cos\theta + \frac{1}{r}\frac{\partial r}{\partial\theta}\sin\theta\right)$$

$$\left.-\frac{1}{\sqrt{1+\cot^2\alpha\sec^2\Psi}}\left(\sin\theta - \frac{1}{r}\frac{\partial r}{\partial\theta}\cos\theta\right)\right] \tag{7}$$

The advantage of using this method is that one source distribution may be used for all angles of attack or yaw and the only variable with the angle is therefore the strength of each source. Furthermore, for small angles the strength of each source will be linearly proportional to the angle of attack or yaw.

Inasmuch as the free stream is no longer in the axial direction relative to the body, the pressure-coefficient relations (equations (5) and (6)) must be revised. These relations become

$$C_p = \frac{2}{\gamma M^2}\left(\left\{1 - \frac{\gamma-1}{2} M^2 \left[2\frac{U_x'}{U} + \left(\frac{U_x}{U}\right)^2 + \left(\frac{U_r}{U}\right)^2 + \left(\frac{U_\theta}{U}\right)^2\right]\right\}^{\frac{\gamma}{\gamma-1}} - 1\right) \tag{8}$$

and

$$C_p = -2\frac{U_x'}{U} \tag{9}$$

where

$$U_x' = \frac{U_x}{\sqrt{\tan^2\alpha + \tan^2\Psi + 1}} + \frac{U_r\cos\theta - U_\theta\sin\theta}{\sqrt{1 + \cot^2\Psi\sec^2\alpha}} + \frac{U_r\sin\theta + U_\theta\cos\theta}{\sqrt{1 + \cot^2\alpha\sec^2\Psi}} \tag{10}$$

The source configurations used to calculate the pressure distribution over the test body are shown in figure 3. For angles of attack and yaw of 0°, sources 1 to 7 were used and the strengths of sources 1 and 7, 2 and 6, and 3 and 5 were respectively equal. These positions were found with the aid of the rules given in reference 6. Instead of putting the source nearest to a peak at the center of curvature of the peak, a better approximation is to place this source at the focus of the peak. This procedure is similar to that sometimes employed in subsonic-flow problems solved by source distributions. For angle of attack, sources 1 to 7 were used with different strengths. For angle of yaw, all the sources were used. In this case, the strengths of sources 1 and 7, 2 and 6, 3 and 5, 8 and 14, 9 and 13, and 10 and 12 were respectively equal. The positions and the number of sources added for yaw were arbitrarily chosen, except that the sources could not be close to the surface. With the exception of this limitation, the accuracy of the solution is insensitive to small changes in the position of sources 8 to 14.

[redacted]

## RESULTS AND DISCUSSION

Experimental data for several angles of yaw and attack are presented in figures 4 and 5. Theoretical calculations based on the linearized theory using equations (8) and (9) for the pressure coefficient are also shown for comparison. The experimental points represent the average of the pressures at corresponding stations on the body. Data were obtained for angles of yaw ranging from $-16^\circ$ to $16^\circ$ and angles of attack from $-10^\circ$ to $10^\circ$. Schlieren observation indicated no shock separation on the cone or interference from the shock caused by the strut over the range of angles of the investigation.

The linearized theory using equation (8) agrees well with the experimental results for moderate angles of yaw (fig. 4). As the angle was increased, the deviation between theory and experiment slightly increased on the compressive side of the cone. On the expansive side the agreement remained good, which is to be expected because an angle of yaw of $6^\circ$ corresponds to zero flow deflection on the midpoint of this side. The increasing variation between theory and experiment with increasing flow angle is also illustrated by the fact that the agreement is best over the slenderest parts of the body, that is, the parts of the body that least disturb the flow.

Comparison of the effects of using the complete equation for the pressure coefficient (equation (8)) with the use of the linearized one (equation (9)) shows that the values predicted by the use of the linearized relation are consistently high, especially when the flow deflection is large.

The linearized theory using equation (8) shows close agreement with experiment throughout the range of angles of attack over which the experiments were conducted (fig. 5). The excellent agreement between theory and experiment at an angle of attack of $10^\circ$, especially at the station $\theta = -90^\circ$ where the flow angle was $28.5^\circ$, indicates that the effect of assuming that the Mach cones follow the body rather than the flow is negligible. The Mach angle corresponding to the experimental Mach number is about $32^\circ$.

The variation of pressure coefficient with angle of attack at a station is predicted very closely by the linearized theory using equation (8) (fig. 6). The linearized relation for the pressure coefficient (equation (9)) did not show nearly as good agreement with experiment, nor did it correctly predict the rate of change

of pressure coefficient with angle of attack over a range of more than a few degrees. Similar results for angle of yaw are illustrated in figure 7, where linearized theory using the complete equation for pressure coefficient (equation (8)) again closely agrees with the experimental data.

The experimental results presented show excellent agreement with the linearized theory using the complete equation for the pressure coefficient (equation (8)). If, however, a similar procedure is used in comparing the linearized solution for a right circular cone with the exact values of reference 7, the results predicted by the linearized theory using the linearized pressure-coefficient relation (equation (9)) show better agreement with the results of Taylor and Maccoll (reference 7) than do those predicted by the complete relation. Because opposite results are obtained for the two cases, even though the same linearized theory is used for both, the excellent agreement between the experimental values for the elliptic cone and the values predicted by the linearized theory may be fortuitous.

## SUMMARY OF RESULTS

The following results were obtained from an investigation of the pressure distribution on a thin conical body of elliptical cross section at a Mach number of 1.89:

1. At moderate angle of flow deflection, the experimental pressure distribution was in close agreement with the linearized theory using the complete equation for pressure coefficient. As the angle of flow deflection increased, the deviation from experiment of the theoretical pressure coefficient increased slightly although agreement was satisfactory over the entire range of calculations.

2. Comparison of the complete equation for pressure coefficient with the equation usually used in connection with the linearized theory indicated that the terms omitted in obtaining the linearized equation were too large to be neglected. Inasmuch as the exact results of Taylor and Maccoll for a right circular cone show better agreement with the linearized theory when the linearized pressure-coefficient relation is used than when the complete relation is applied, whereas the opposite result was obtained in comparing the experimental results in this report with the linearized theory, the excellent agreement between the linearized theory and the experimental results presented may be fortuitous.

Lewis Flight Propulsion Laboratory,
National Advisory Committee for Aeronautics,
Cleveland, Ohio.

[redacted]

REFERENCES

1. von Kármán, Theodor, and Moore, Norton B.: Resistance of Slender Bodies Moving with Supersonic Velocities, with Special Reference to Projectiles. Trans. A.S.M.E., vol. 54, no. 23, Dec. 15, 1932, pp.303-310.

2. Tsien, Hsue-Shen: Supersonic Flow over an Inclined Body of Revolution. Jour. Aero. Sci., vol. 5, no. 12, Oct. 1938, pp.480-483.

3. Brown, Clinton E., and Parker, Hermon M.: A Method for the Calculation of External Lift, Moment, and Pressure Drag of Slender Open-Nose Bodies of Revolution of Supersonic Speeds. NACA Rep. No. 808, 1945.

4. Ferri, Antonio: Supersonic-Tunnel Tests of Projectiles in Germany and Italy. NACA ACR No. I5H08, 1945.

5. Sauer, R.: Method of Characteristics for Three-Dimensional Axially Symmetrical Supersonic Flows. NACA TM No. 1133, 1947.

6. Maslen, Stephen H.: Method for Calculation of Pressure Distributions on Thin Conical Bodies of Arbitrary Cross Section in Supersonic Stream. NACA TN No. 1659, 1948.

7. Taylor, G. I., and Maccoll, J. W.: The Air Pressure on a Cone Moving at High Speeds. - I and II. Proc. Roy. Soc. (London), ser. A, vol 139, no. 838, Feb. 1, 1933, pp.278-311.

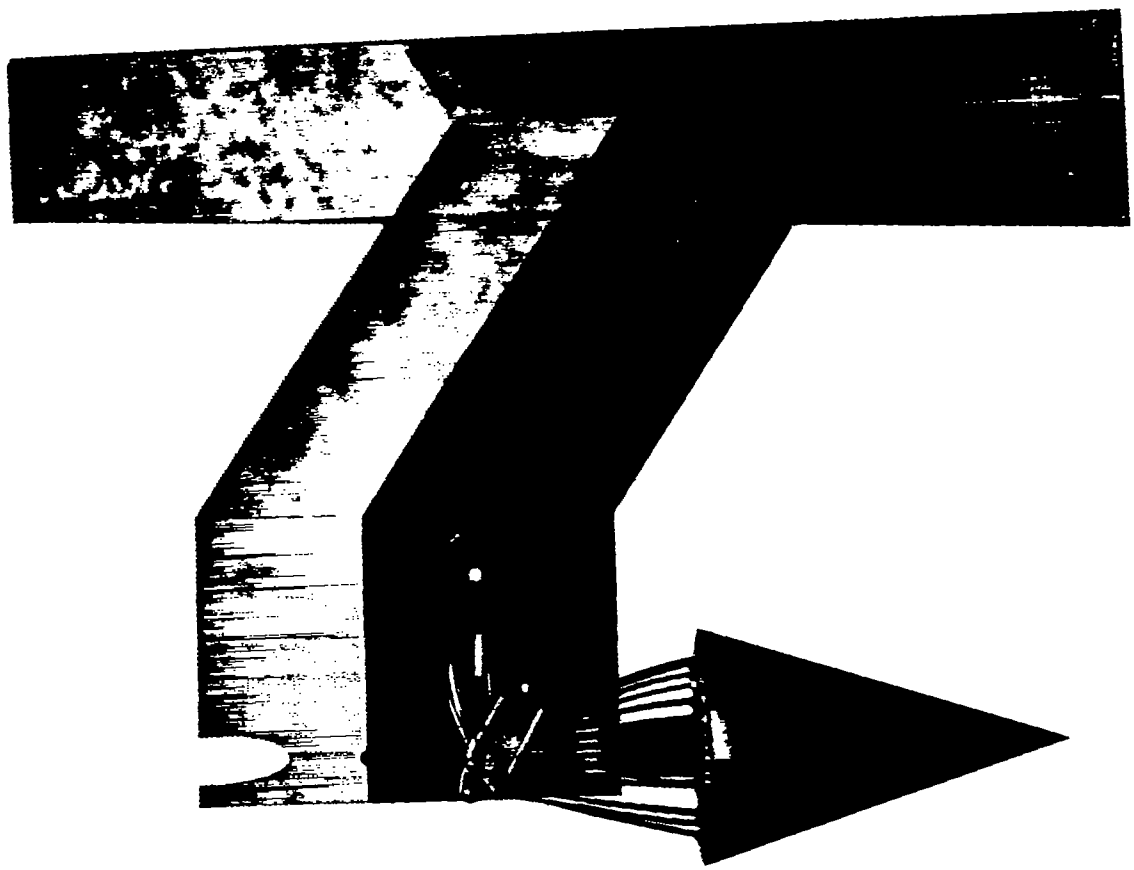

NACA

C-21730
6-23-48

Figure 1. - Cone mounted on support body.

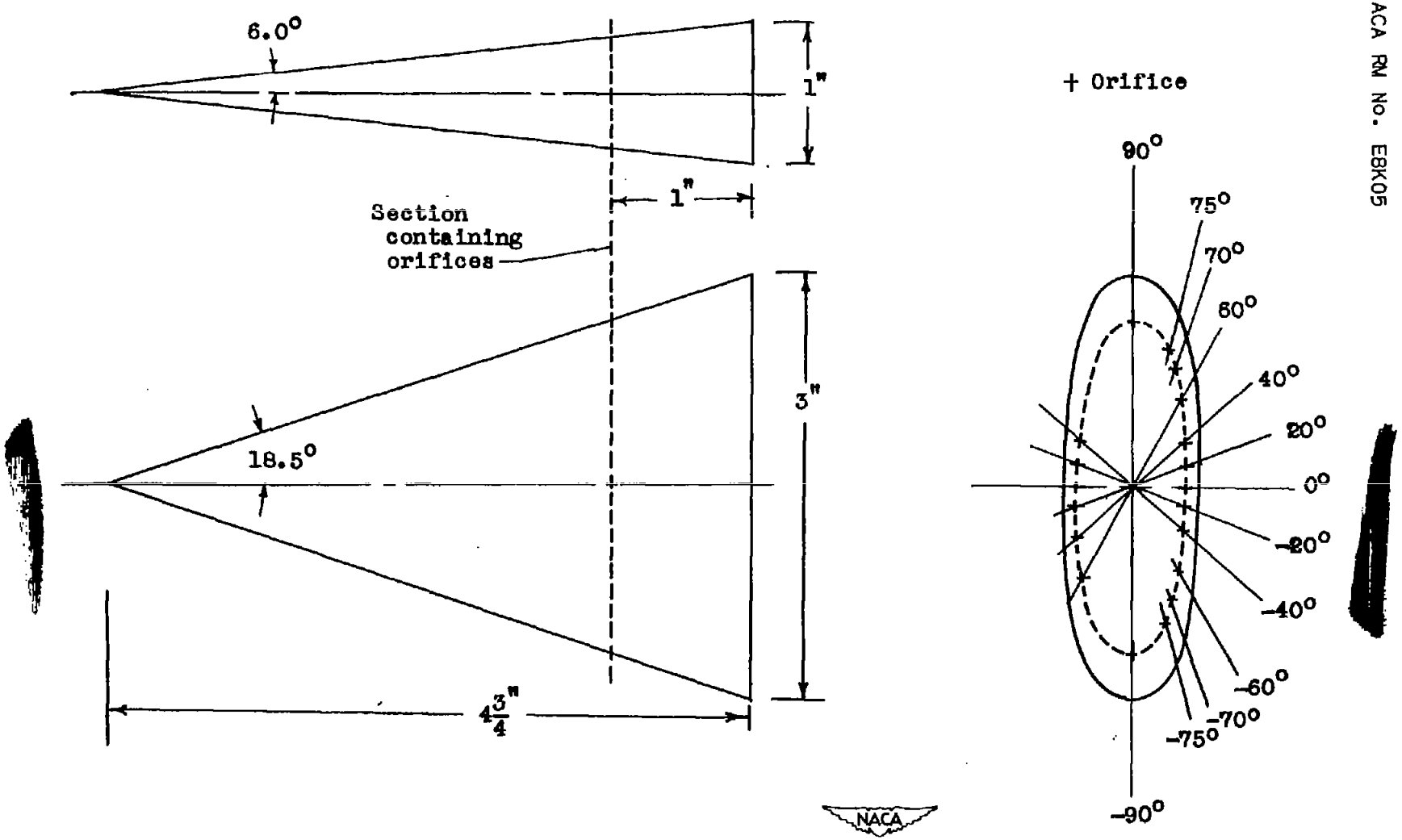


Figure 2. - Sketch of model showing orifice positions and important dimensions.

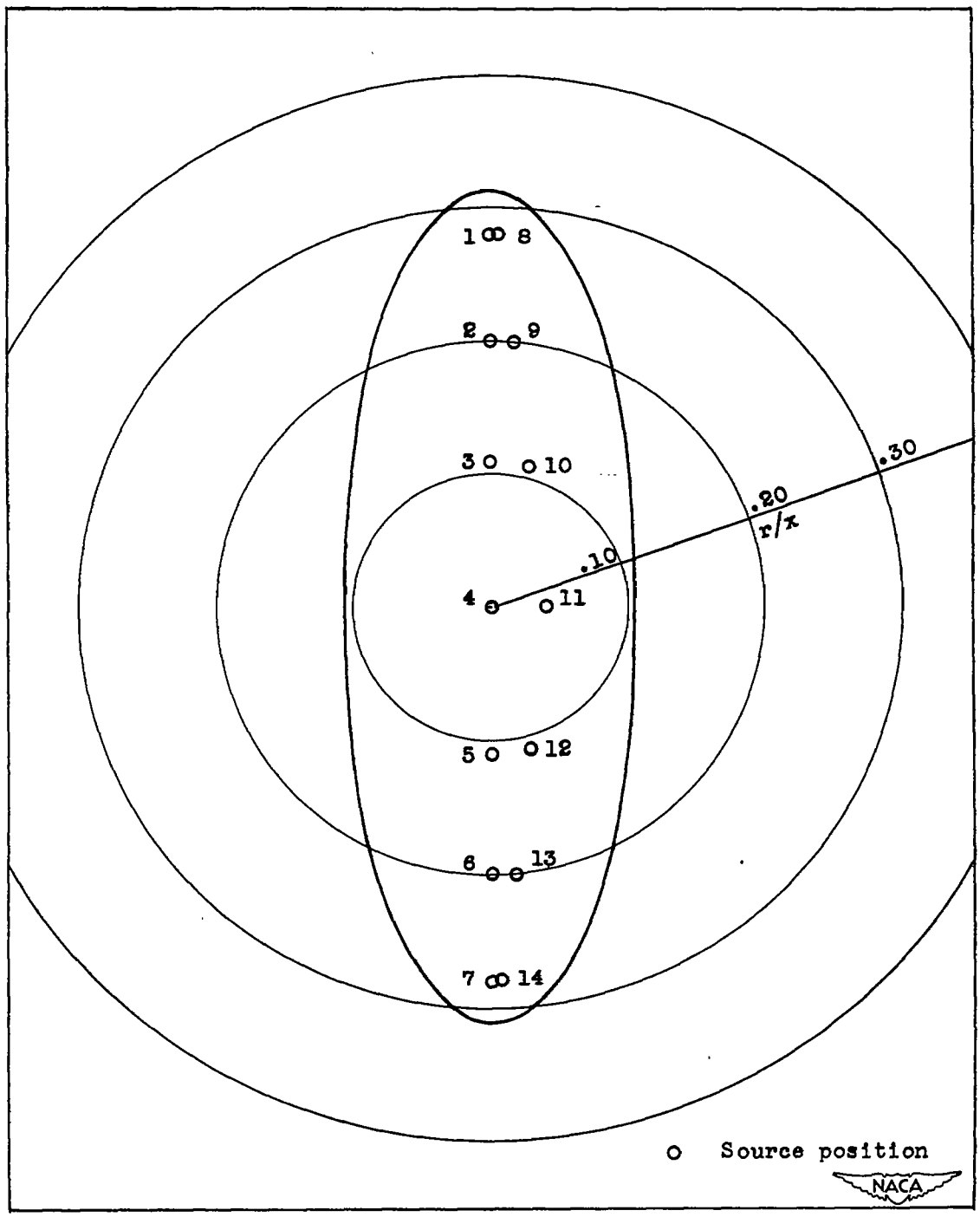


Figure 3. - Cross section of test body showing source configuration for theoretical calculations.

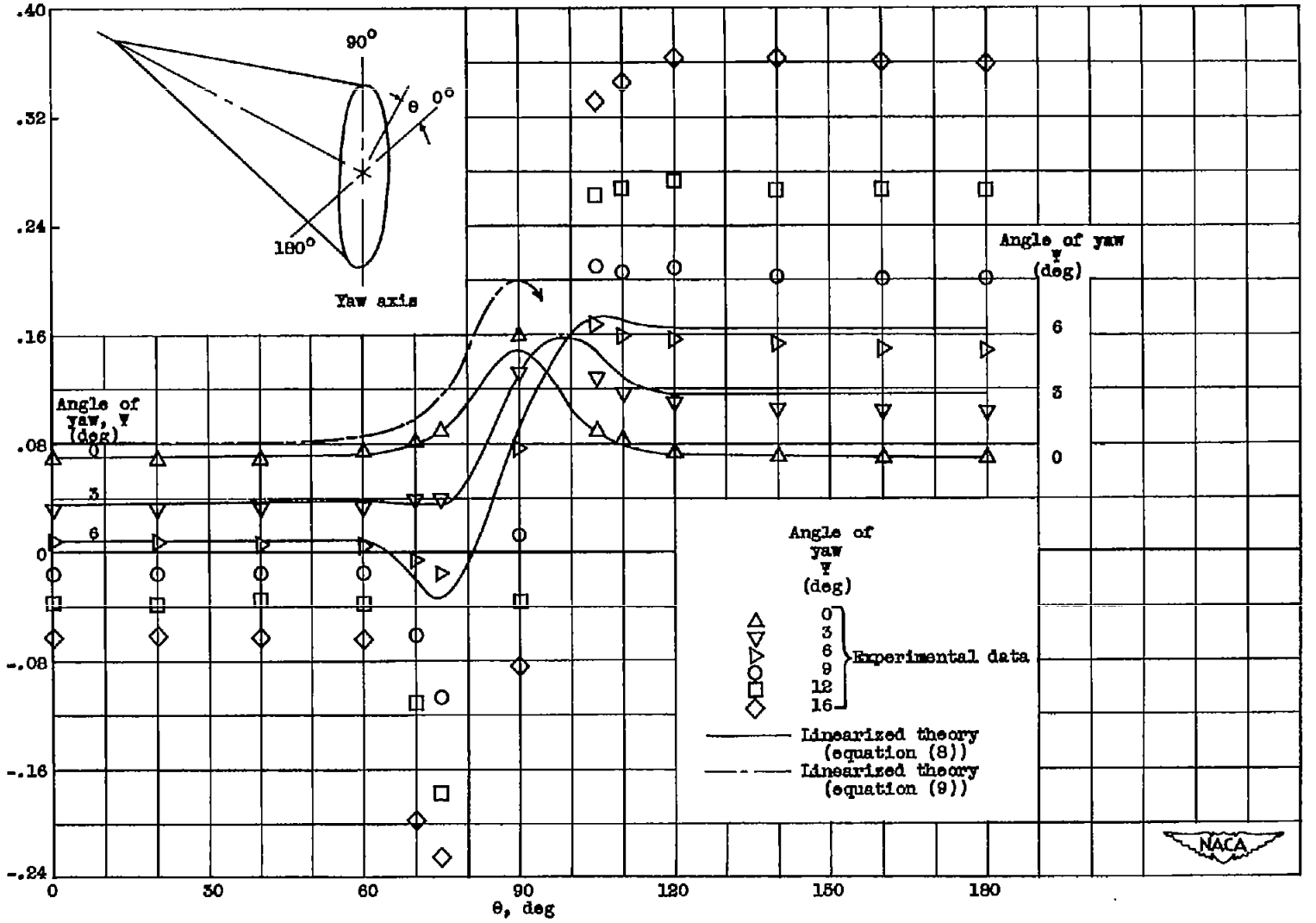


Figure 4. - Variation of pressure coefficient with position on model at an angle of attack of 0°.

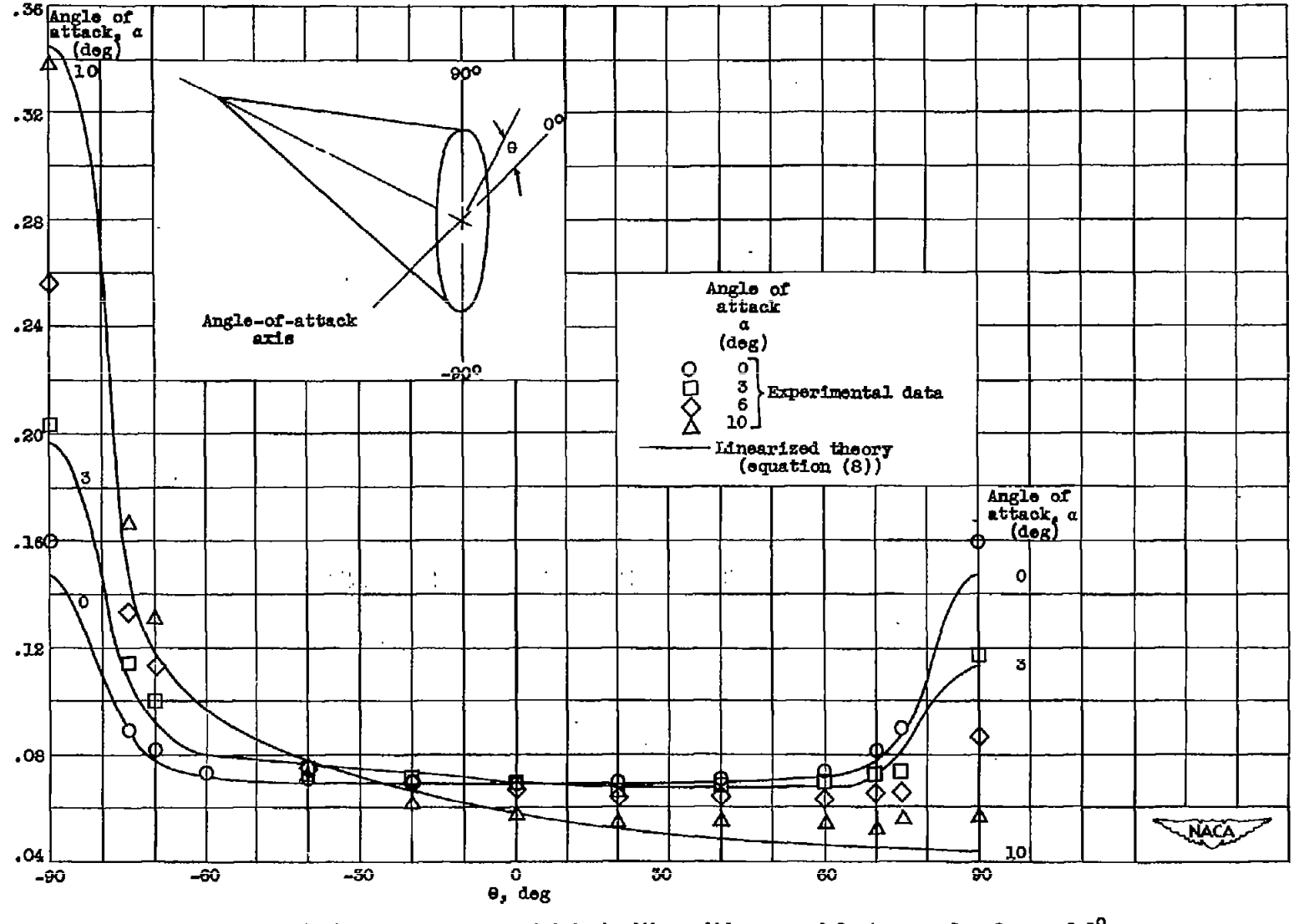


Figure 5. - Variation of pressure coefficient with position on model at an angle of yaw of 0°.

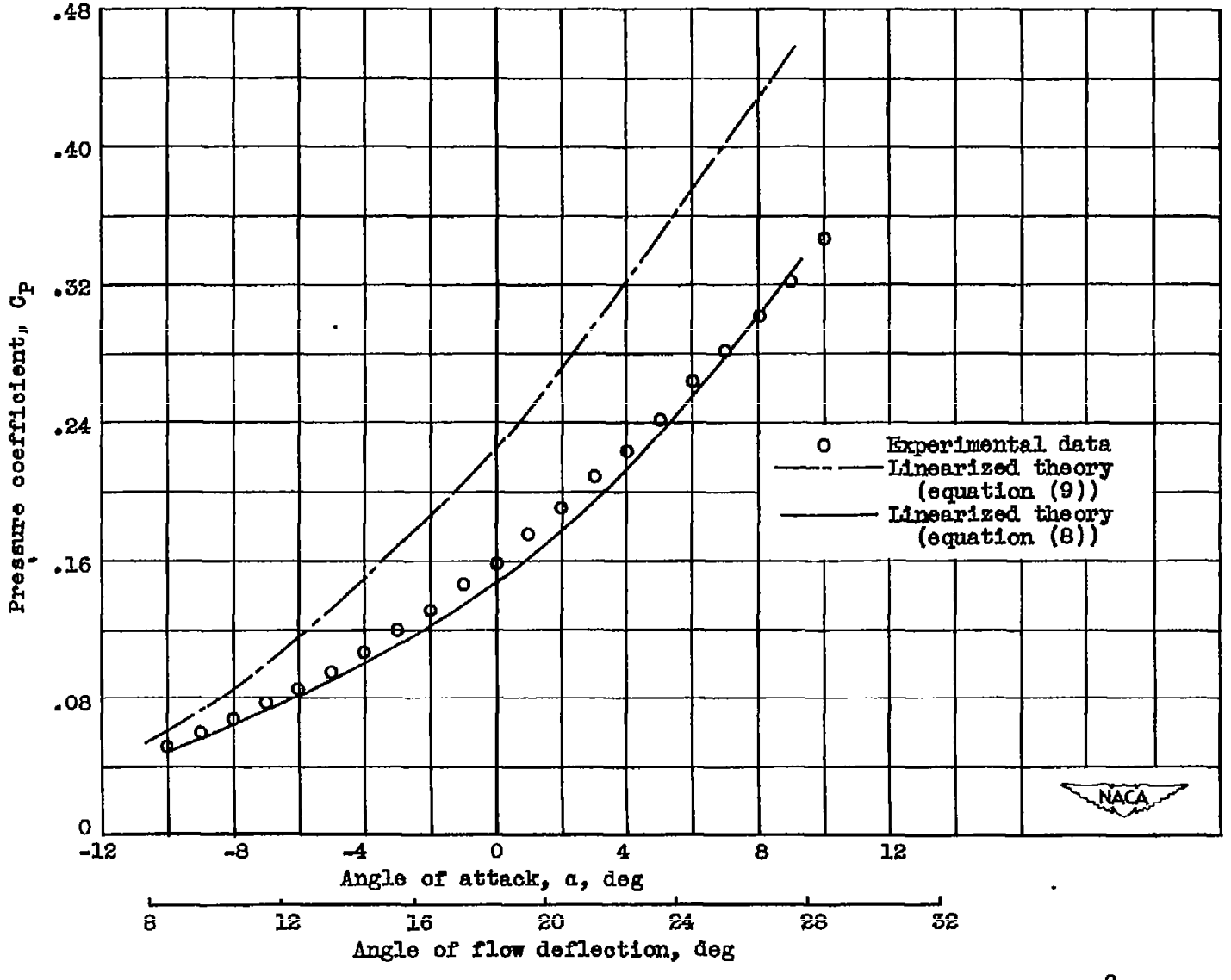


Figure 6. - Variation of pressure coefficient with angle of attack for θ of ±90°.

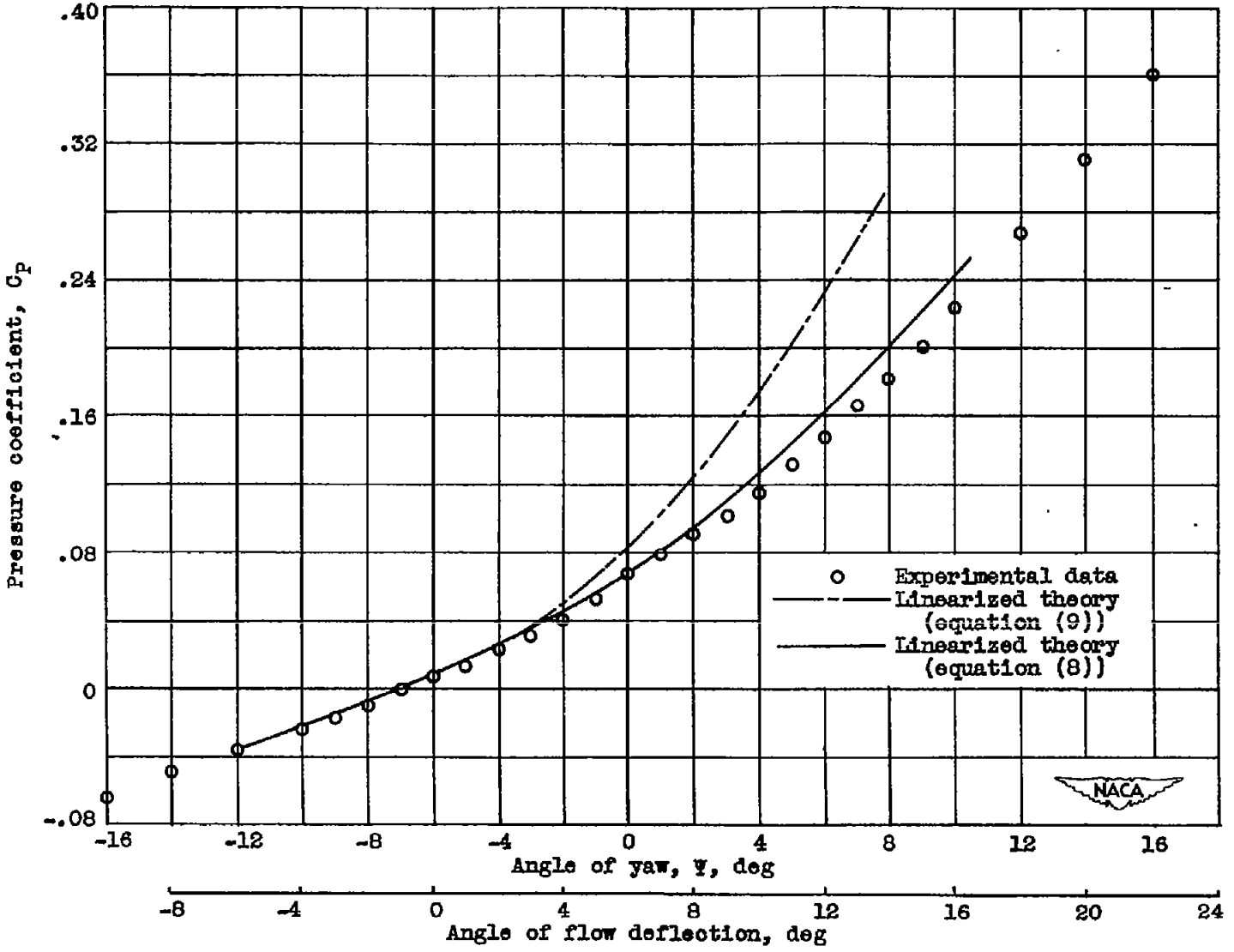


Figure 7. - Variation of pressure coefficient with angle of yaw for $\theta$ of 180°.